

STRUCTURAL ANALYSIS OF  
177-FA REDESIGNED SURVEILLANCE  
SPECIMEN HOLDER TUBE

564 087

7908020516

**Babcock & Wilcox**

17908020516

83

STRUCTURAL ANALYSIS OF  
177-FA REDESIGNED SURVEILLANCE  
SPECIMEN HOLDER TUBE

by

C. W. Pryor  
D. E. Thoren  
G. J. Vames  
R. J. Harris

BABCOCK & WILCOX  
Power Generation Group  
Nuclear Power Generation Division  
P. O. Box 1260  
Lynchburg, Virginia 24505

564 008



UNITED STATES  
NUCLEAR REGULATORY COMMISSION  
WASHINGTON, D. C. 20555

J. H. Taylor

APR 11 1979

APR 4 1979

Mr. James H. Taylor  
Manager, Licensing  
Babcock & Wilcox Company  
Nuclear Power Generation  
P. O. Box 1260  
Lynchburg, Virginia 24505

Dear Mr. Taylor:

SUBJECT: EVALUATION OF BAW-10051, SUPPLEMENT 1

We have completed our evaluation of Babcock & Wilcox Topical Report BAW-10051, Supplement 1, "Design of Reactor Internals and Incore Instrument Nozzles for Flow Induced Vibration - Structural Analysis of 177-FA Redesign Surveillance Specimen Holder Tube." We have determined that BAW-10051, Supplement 1, is acceptable for reference to describe the modified surveillance specimen holder tube design for B&W 177-FA plants.

If our criteria or regulations change, such that our conclusions concerning BAW-10051, Supplement 1, are invalidated, we will notify you and provide you with an opportunity to revise and, if you desire, resubmit this report for our review.

We request, that within three months, you issue a revised version of BAW-10051, Supplement 1, incorporating this letter.

Sincerely,

A handwritten signature in dark ink, appearing to read "Steven A. Varga".

Steven A. Varga, Chief  
Light Water Reactors Branch No. 4  
Division of Project Management

cc: Mr. Robert B. Borsum  
7735 Old Georgetown Road  
Bethesda, Md. 20014

564 089

Babcock & Wilcox  
Power Generation Group  
Nuclear Power Generation Division  
Lynchburg, Virginia

Topical Report BAW-10051A, Supplement 1  
June 1979

Structural Analysis of 177-FA Redesigned  
Surveillance Specimen Holder Tube

C. W. Pryor, D. E. Thoren, G. J. Vames, R. J. Harris

Key Words: Internals, Surveillance Specimen Holder Tubes,  
Temperature, Flow-Induced Loads, Stresses

ABSTRACT

Because of inservice operational problems, the surveillance specimen holder tubes described in B&W topical report BAW-10051 have been redesigned. This report describes the new design and structural analysis for normal operation and upset loading conditions. The results of the analysis demonstrate the adequacy of the new surveillance specimen holder tubes for their design life of 40 years.

564 090

CONTENTS

	Page
1. INTRODUCTION . . . . .	1-1
2. SUMMARY AND CONCLUSIONS . . . . .	2-1
3. DESIGN DESCRIPTION . . . . .	3-1
3.1. Functional Description . . . . .	3-1
3.2. Mechanical Description . . . . .	3-1
4. DESIGN CRITERIA FOR HEAT TRANSFER AND STRUCTURAL ANALYSIS . . . . .	4-1
5. ANALYSIS . . . . .	5-1
5.1. Heat Transfer . . . . .	5-1
5.1.1. Surveillance Specimen Temperatures . . . . .	5-1
5.1.2. Temperature Distributions for Thermal Stress Analysis . . . . .	5-3
5.2. Finite Element Model . . . . .	5-3
5.3. Natural Frequencies and Mode Shapes . . . . .	5-4
5.4. Vibration Loadings . . . . .	5-4
5.4.1. Random Pressure Fluctuations . . . . .	5-6
5.4.2. Periodic Pressure Fluctuations . . . . .	5-6
5.4.3. Vortex Shedding . . . . .	5-8
5.4.4. Thermal Shield Excitation . . . . .	5-10
5.4.5. Endurance Limit Analysis . . . . .	5-10
5.5. Seismic Loadings . . . . .	5-11
5.6. Normal and Upset Condition Stress Analysis . . . . .	5-11
5.6.1. Steady-State Stresses . . . . .	5-11
5.6.2. Vibrational Stresses . . . . .	5-12
REFERENCES . . . . .	A-1

List of Tables

5-1. Summary of Temperatures in SSHT-Related Components . . . . .	5-13
5-2. SSHT Modal Analysis Results . . . . .	5-14
5-3. Maximum RMS Modal Displacements for SSHT Assembly Due to Random Excitation . . . . .	5-14

Tables (Cont'd)

	Page
5-4. Pressure Flucuations Measured in Five-Vane Bingham Pump Test Loop . . . . .	5-15
5-5. Periodic Pressure Fluctuations Used in SSHT Analysis . . . . .	5-16
5-6. Structural Excitation From Thermal Shield . . . . .	5-17
5-7. Steady-State Primary Plus Secondary Stresses . . . . .	5-17
5-8. Steady-State Peak Stresses . . . . .	5-18
5-9. Stresses Due to Random Vibration Loadings . . . . .	5-18
5-10. Stresses Due to Periodic Pump Pressure Loadings . . . . .	5-19

List of Figures

2-1. Redesigned SSHT Assembly Arrangement . . . . .	2-2
2-2. Flexible Support Brackets for SSHT . . . . .	2-3
4-1. Design Fatigue Curve for Redesigned SSHT . . . . .	4-2
5-1. 177-FA Pressure Vessel Temperature Distribution Due to Gamma Heating . . . . .	5-20
5-2. Surveillance Specimen Configurations . . . . .	5-21
5-3. Surveillance Specimen Temperature Study . . . . .	5-22
5-4. Surveillance Specimen Surface Temperature Vs Flow Velocity . . . . .	5-23
5-5. Temperature Distribution in 177-FA Thermal Shield, $\theta = 11^\circ$ . . . . .	5-24
5-6. Temperature Distribution in 177-FA Thermal Shield, $\theta = 26.5^\circ$ . . . . .	5-25
5-7. Finite Element Beam Model of SSHT and Support Brackets . . . . .	5-26
5-8. Finite Element Beam Model of SSHT Support Brackets . . . . .	5-27
5-9. First Fundamental Mode Shape of SSHT and Capsules . . . . .	5-28
5-10. Second Fundamental Mode Shape of SSHT and Capsules . . . . .	5-28
5-11. Random Pressure Loading Functions . . . . .	5-29
5-12. Superposition of Pump Pressure Wave on SSHT . . . . .	5-30
5-13. Dispersion of Pump Pressure Pulsation at Reactor Vessel Inlet . . . . .	5-31
5-14. Design Crossflow Velocity Distribution for Redesigned 177-FA SSHT . . . . .	5-32
5-15. Results of Endurance Limit Analysis of 177-FA SSHT . . . . .	5-33

564 092

## 1. INTRODUCTION

Operational problems with the design of the surveillance specimen holder tubes (SSHTs) on Babcock & Wilcox's 177-fuel assembly plants necessitated a redesign of the holder tube, as described in B&W topical report BAW-10051<sup>1</sup>.

This report provides a description of the new design in sections 2 and 3, the specified criteria for the structural analysis in section 4, the normal operation and upset loading conditions in section 5, and a comparison of analytical results with the allowable values given in the ASME Code, Section III, Subsection NG for Core Support Structures.

The redesigned SSHT is shown, through extensive analysis and stringent acceptance criteria, to be structurally adequate for the 40-year design life of the 177-fuel assembly plants.

564 093

## 2. SUMMARY AND CONCLUSIONS

This report describes the extensive thermal and mechanical analyses performed to demonstrate the acceptability of the new design of the 177-fuel assembly surveillance specimen holder tube (SSHT) assembly. The new design is illustrated schematically in Figure 2-1. Its major components include surveillance specimen capsules with wedged end fittings, a surveillance holder tube, rigid and flexible support brackets (Figure 2-2), and a locking mechanism that wedges the capsules within the surrounding holder tube.

The design criteria for the SSHT were established on the basis of functional requirements and structural integrity. The functional aspects of the design were satisfied by ensuring that specimens will be exposed to the proper thermal and neutron environment. The structural integrity was confirmed through extensive steady-state and vibrational analyses in which results were compared with the conservative limits given in the ASME Code, Subsection NG for Core Support Structures. The fatigue analysis, which must consider the small amplitude, high-cycle vibrational stresses, was based on conservative cumulative damage and the associated fatigue design curve.

The results of the analytical studies indicate that the new design for the SSHT will be adequate for the 40-year design life of the nuclear plant. Absolute deformations are expected to be extremely small; there should be no relative deformation between parts at their structural interfaces, and calculated stresses are within Subsection NG allowable limits.

564 094

Figure 2-1. Redesigned SSHT Assembly Arrangement

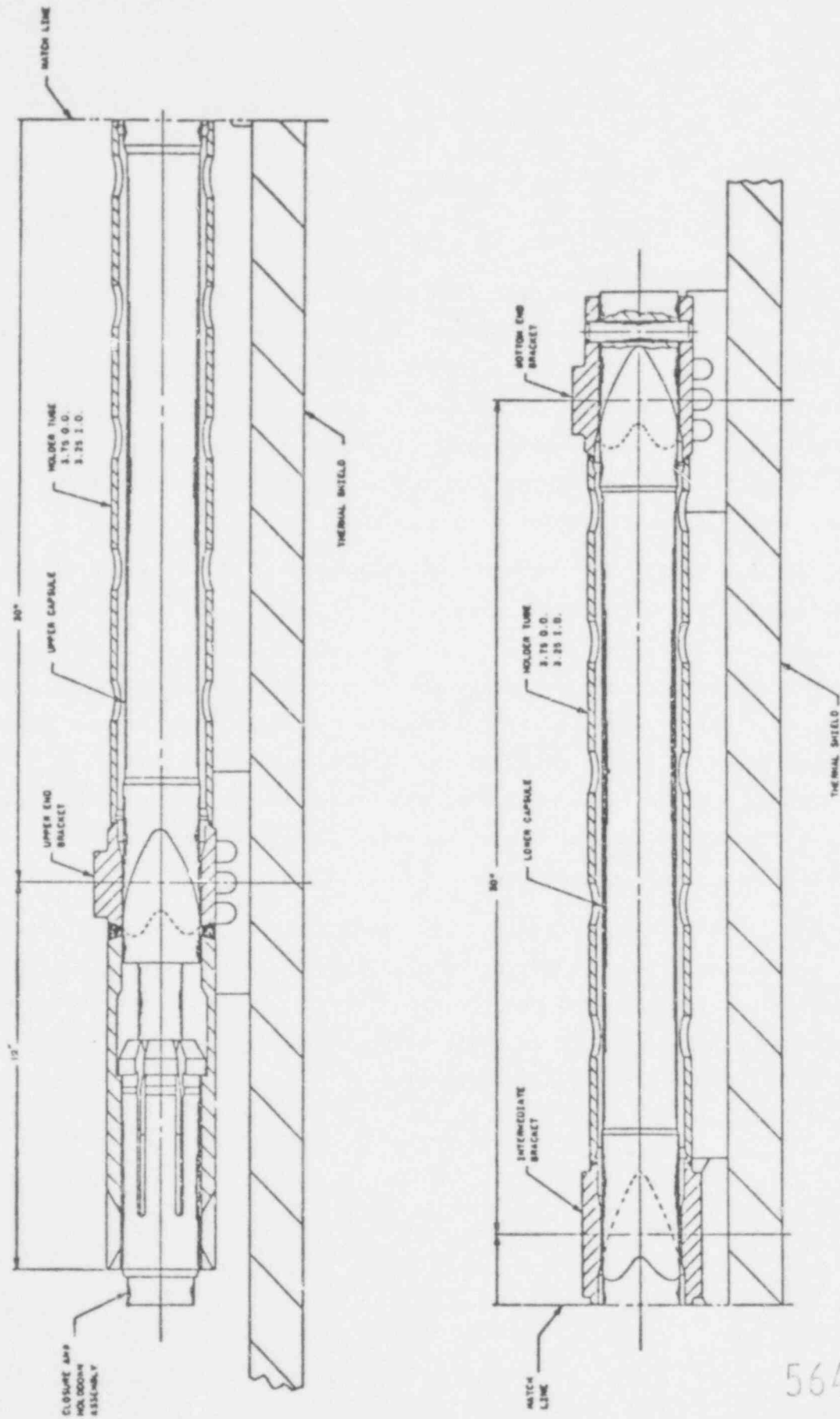
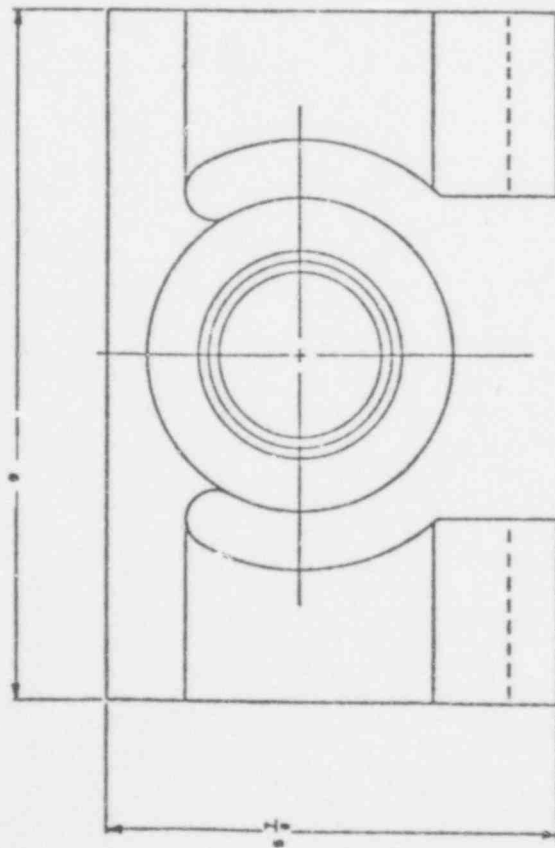
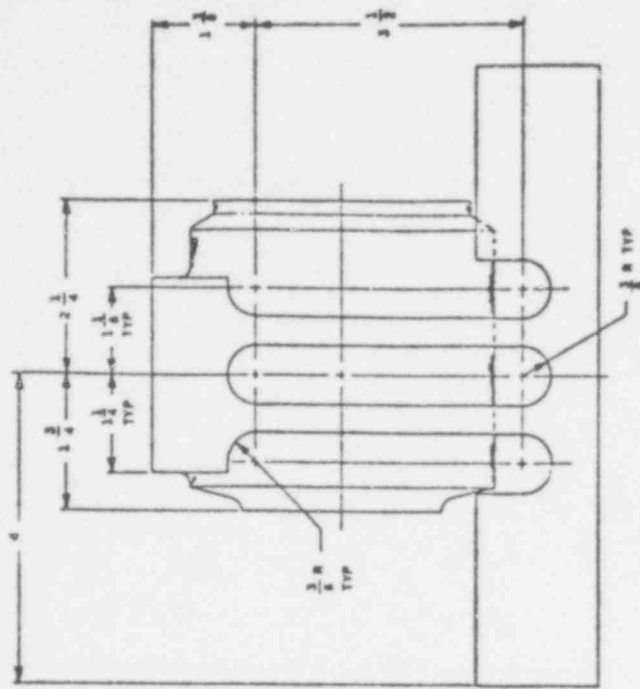


Figure 2-2. Flexible Support Brackets for SSHT



564 096

### 3. DESIGN DESCRIPTION

The new design of the 177-fuel assembly SSHT is illustrated in Figures 2-1 and 2-2. The functional and mechanical descriptions of the new design follow, and the relevant design criteria are included in section 4.

#### 3.1. Functional Description

The SSHT is designed to house the samples or specimens of reactor vessel base metal and weld metal in a representative thermal and neutron environment. The holder tube is positioned in the reactor downcomer annulus, azimuthally and radially away from the core's major axis to ensure that this requirement is satisfied.

#### 3.2. Mechanical Description

The new SSHT assembly consists of surveillance specimen capsules, a surveillance specimen holder tube, and brackets that connect the assembly to the reactor internal thermal shield. As shown in Figure 2-1, the surveillance specimen holder structure has two spans, each 30 inches long. The upper 12-inch cantilevered section of the tube houses a locking mechanism, which wedges the surveillance capsules against the surrounding holder tube.

Because the tube is attached to the thermal shield, it must be designed to accommodate differential thermal expansion. Thus, the tube is attached at its mid-height with a rigid bracket and at each end with "flexible" brackets. These brackets, illustrated in Figure 2-2, are flexible only axially and are designed to allow the shield to grow thermally without transmitting the corresponding deformations to the SSHT. All brackets are stiff in the radial and tangential directions to provide support for flow-induced vibration loadings. The brackets are attached to the thermal shield with 0.75-inch, high-strength bolts.

The surveillance capsules are packed with specimens having an outer diameter of 2.75 inches and extending over a length of 30 inches. The capsules have

564 007

double-action wedged end fittings so that when they are stacked inside the SSHT, they can be wedged against it through the application of a compressive preload from the locking mechanism above. Following capsule handling, this mechanism is activated by a torque wrench and jackscrew, which puts the capsules in compression and the holder tube in tension.

564 028

#### 4. DESIGN CRITERIA FOR HEAT TRANSFER AND STRUCTURAL ANALYSIS

The new design of the SSHT will be subjected to steady-state thermal and mechanical loadings and low- and high-cycle vibrational loadings. To successfully demonstrate the structural integrity of the new design, certain criteria have been established for its acceptance. This section describes the SSHT design criteria, which also contain functional requirements which the new design must satisfy.

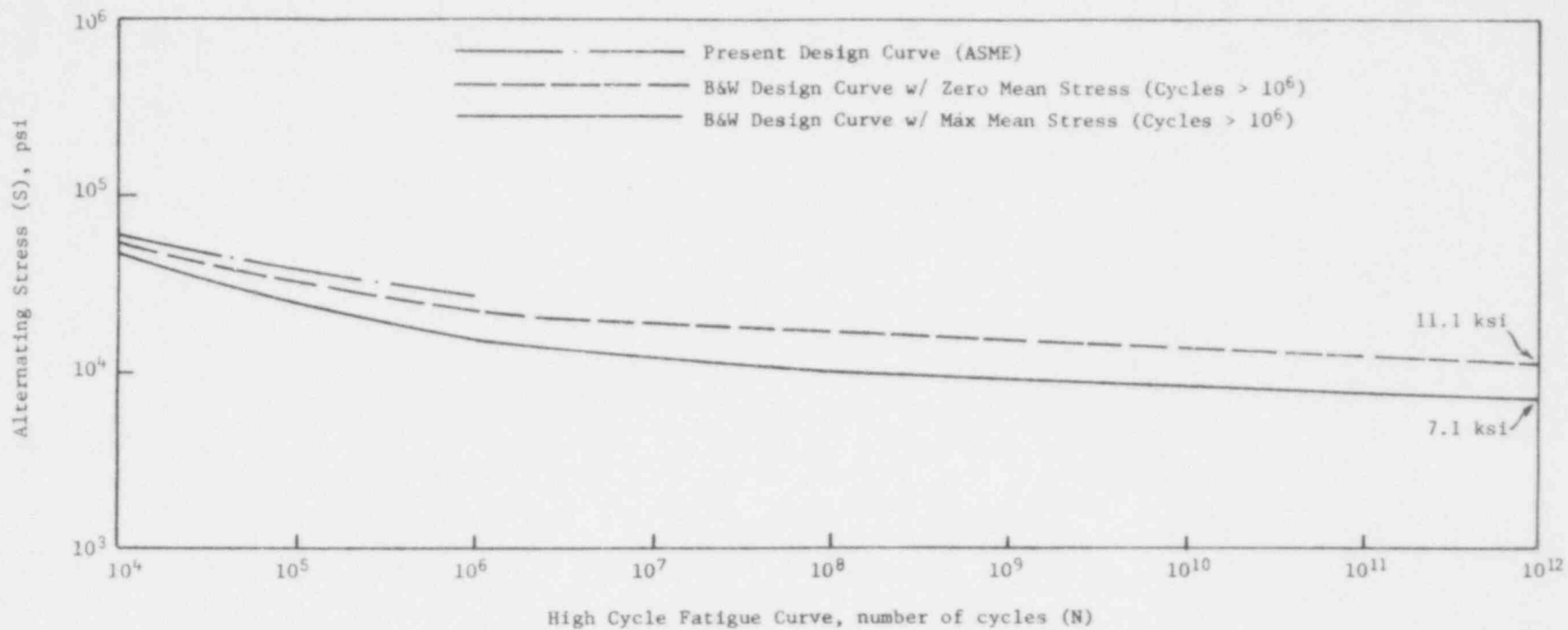
To meet the surveillance program requirement., the capsules must be positioned in the downcomer annulus so that the specimen temperatures are within  $\pm 25\text{F}$  of the temperature at the  $1/4$  thickness location in the reactor vessel wall. They also must be located axially within  $\pm 60$  inches of the core midplane. This ensures that the specimens are subjected to representative neutron fluence levels.

With the SSHTs attached to the thermal shield and protruding into the reactor downcomer annulus, the tubes will be subjected to cross flow- and parallel flow-induced loadings. The maximum specified cross flow and parallel flow velocities are 26 and 50 fps, respectively.

The SSHT assembly is designed and analyzed in accordance with the ASME Code, Section III, Subsection NG for Core Support Structures. In particular, the loadings specified for normal operating and upset conditions are considered in the analysis. The resultant stresses from the loading conditions are compared with Code limits to ensure structural integrity.

As indicated in B&W topical report BAW-10051<sup>1</sup>, the consideration of high-cycle, flow-induced vibration stresses requires a fatigue evaluation other than that provided in the ASME Code. B&W has developed an extremely conservative S-N design curve for fatigue analysis. The curve, shown in Figure 4-1, includes the effects of mean stress and provides allowable alternating stresses up to  $10^{12}$  cycles. The ASME Code curve, which extends only to  $10^6$  cycles, is also shown for comparison. The design curve in Figure 4-1 is used for computing cumulative usage factors and evaluating the integrity of the SSHT for cyclic loadings.

Figure 4-1. Design Fatigue Curve for Redesigned SSHT



4-2

Babcock & Wilcox

564 100

## 5. ANALYSIS

The new SSHT design and the criteria governing its analysis are described in the preceding sections. This section describes the thermal and structural analyses of the tube and presents detailed numerical results, which are shown to satisfy the acceptance criteria defined in section 4.

### 5.1. Heat Transfer

The heat transfer analysis of the SSHT assembly has two basic objectives:

1. To determine the temperatures of the various surveillance specimens and ensure that they are within  $\pm 25F$  of the  $1/4$  thickness reactor vessel wall temperature.
2. To determine the temperature distributions in all pertinent subcomponents (thermal shield, SSHT, surveillance capsules, and surveillance specimens) to facilitate a thermal stress analysis of the entire assembly.

The heat transfer analysis requires knowledge of the gamma heating distributions in the affected components and knowledge of pertinent reactor coolant conditions. Two azimuthal locations are possible for the redesigned SSHTs: one is  $11^\circ$  away from the plane containing the major core axis, and the other is  $26.5^\circ$  away. The temperature distributions are determined using classical methods of axis-symmetric heat transfer analysis, where the gamma heating serves as the volume heat input and the reactor coolant parameters of temperature and velocity are converted to surface boundary conditions. The major axis gamma heating is scaled by a peaking factor to account for the azimuthal location of the holder tube assembly being analyzed.

#### 5.1.1. Surveillance Specimen Temperatures

To ensure that the surveillance specimens are within  $\pm 25F$  of the  $1/4$  thickness reactor vessel wall temperature, an analysis of the reactor vessel was conducted. Figure 5-1 shows the computed temperature distribution through the thickness of the reactor vessel wall. A maximum temperature of 576F is noted, along with a

1/4 thickness temperature of 572F. Several reactor vessel cladding thicknesses were considered in the analysis and did not significantly perturb the distribution shown in Figure 5-1. Thus, the surveillance specimen temperatures must be within the range from 597 to 547F ( $\pm 25$ F of the 1/4 thickness vessel wall temperature).

Two types of surveillance specimens were analyzed; these are shown in Figure 5-2. The Charpy impact specimens are packed inside the surveillance capsules (0.125-inch wall, stainless steel tubes) with powdered aluminum. They are arranged in a square, 4 by 4 array with 0.005-inch helium gaps between specimens. This configuration has poor heat transfer characteristics because of the high resistance associated with the helium gaps; its temperature will tend to be on the high side of the allowable range. Thus, for a conservative analysis, it is located at the  $\theta = 11^\circ$  azimuthal location, which has the highest peaking factor, 1.19.

The uniaxial tension specimens are 0.375-inch rods which are also packed inside the surveillance capsules with powdered aluminum. These specimens are arranged in a square 2 by 2 array with large aluminum spaces between specimens. This configuration has good heat transfer characteristics because of the large percentage of aluminum in the cross section. Its temperature will tend to be on the low side of the allowable range. Thus, for a conservative analysis, it is located at the  $\theta = 26.5^\circ$  azimuthal position, which has the lowest peaking factor, 0.83.

Figure 5-3 illustrates the resultant temperature distributions in the two types of surveillance specimen configurations analyzed. The Charpy specimens vary from a maximum temperature of 578F in the interior region to a minimum of 568F in the exterior region. The tensile specimens are cooled more adequately and vary slightly in temperature from a maximum of 558F to a minimum of 556F. All these temperatures are within the allowable range, and the criterion for specimen temperatures is satisfied.

Figure 5-4 indicates that a coolant velocity of 1 fps was assumed in the annulus between the surveillance capsules and the holder tube. This is an extremely conservative assumption since the velocity outside the highly perforated SSHT is 22 fps. Figure 5-4 shows that the assumption of coolant velocity does not have a significant effect on the capsule boundary conditions unless it drops below 0.5 fps, where turbulent flow is not ensured. Thus, the analysis of the

564 102

surveillance specimen has been conducted using a conservative assumption for reactor coolant velocity distribution.

#### 5.1.2. Temperature Distributions for Thermal Stress Analysis

Figures 5-5 and 5-6 show the calculated temperature distributions in the 177-FA thermal shield to which the SSHTs will be attached. Figure 5-5 shows the temperatures at the  $\theta = 11^\circ$  azimuthal location, and Figure 5-6 shows those at  $\theta = 26.5^\circ$ . These temperature distributions are applicable over the entire height of the SSHT because of the flatness of the gamma heating profile.

Table 5-1 summarizes the average and maximum temperatures in all structural components related to the SSHT assembly. As indicated, the tube itself maintains a constant temperature equal to that of the reactor coolant. This is a result of the thorough exposure of both the inner and outer surfaces to coolant flow. These temperature distributions form the necessary input for computing thermal stresses in all affected components. The thermal stress analysis and results are described later.

#### 5.2. Finite Element Model

A finite element model was developed to analyze the SSHTs and capsules for thermal and vibration loadings. The model consists of discrete beam elements representing the SSHT, capsules, and support brackets. The model was developed for processing by the NASTRAN computer code, which is a public domain, large-scale, finite element program.

Figures 5-7 and 5-8 show the finite element modeling of the SSHT, capsules, and support brackets. The model is assumed to be rigidly supported where the brackets are bolted to the thermal shield. The tube and capsules are modeled with beam elements having a length of 3 inches. The capsule and tube elements are coincident over the lower 60-inch length and behave independently except where they are continuously attached to the support brackets. The perforations in the holder tube are incorporated in the computation of the effective mass and stiffness of the representative beam elements. As indicated in Figure 5-7, the SSHT extends 12 inches above the uppermost support bracket.

The flexible end brackets were modeled as shown in Figure 5-8. The bracket legs were modeled with beam elements, which were connected to the tube model centerline with rigid bars. The very rigid intermediate support bracket was modeled

with three simple supports spanning its 6-inch height. These supports constrain local translational deformations but permit limited coupling between the overall behavior of the upper and lower spans.

### 5.3. Natural Frequencies and Mode Shapes

The natural frequencies of the SSHT, in the range of interest, were determined using the NASTRAN computer code and the finite element model described in the preceding section. Natural frequencies are of interest from the standpoint of their proximity to excitational frequencies. They are the basic ingredient for characterizing the behavior of structures subjected to dynamic excitation.

The effects of water on the natural frequencies were accounted for by adding virtual mass to the model in accordance with reference 2. The tube perforations were accounted for by reducing the virtual mass by the ratio of the surface area of the perforations to the surface area of the unperforated tube.

The natural frequencies and mode shapes of the model in the radial and circumferential directions relative to the thermal shield were computed. The frequency results are tabulated in Table 5-2. Figures 5-9 and 5-10 illustrate the mode shapes corresponding to the two lowest natural frequencies, 204 and 219 Hz.

All the frequencies computed are above 200 Hz, and the model is seen to behave in a representative beamlike fashion. Vortex shedding frequencies are normally less than 50 Hz in the vicinity of the SSHT, and the design is considered satisfactory from the standpoint of separation of structural frequencies and shedding frequencies.

### 5.4. Vibration Loadings

This section describes the vibration loadings considered in the analysis of the redesigned SSHTs. The sources of vibrational excitation imparted to the holder tube have two forms: hydraulic and structural. An extensive examination of the hydraulic environment in the vicinity of the holder tube assembly has identified the following loading mechanisms:

1. Random pressure fluctuations (turbulent flow in downcomer annulus).
2. Periodic pressure fluctuations (characterized at pump blade passing frequencies).
3. Vortex shedding pressure fluctuations.

564 104

The structural excitation consists of motion imparted to the SSHT assembly from the vibration of the thermal shield to which it is attached.

These hydraulic and structural vibration loading mechanisms are discussed in detail in the following paragraphs. An endurance limit or "brute force" analysis, in which all vibrational loadings are considered as proportional to the dynamic head, is also presented.

#### 5.4.1. Random Pressure Fluctuations

The SSHT will respond to the non-homogeneous random pressure fluctuations caused by turbulent flow adjacent to the structure. The method of analysis is to define the loading function statistically with a pressure power spectral density (PSD), which is applied to an analytical model of the SSHT. The theory for analysis has been developed by B&W and translated into a computer program that calculates RMS displacements as a function of position. The parameters chosen for analysis of the SSHT will provide conservative responses for random vibration. The results of random vibration analysis are in terms of RMS displacements at the natural frequencies of the SSHT in water. This displacement configuration can then be translated into stresses in the component parts of the SSHT assembly. The random pressure loading used for design purposes is shown in Figure 5-11. It is based on an empirical relationship between dynamic pressure and mean square pressure ( $\bar{p}^2$ ). The dynamic pressure is given by

$$q = \frac{1}{2} \rho V^2$$

where  $\rho$  = fluid density and  $V$  = design velocity.

A report by J. Clinch<sup>3</sup> indicates that the ratio between  $q^2$  and  $\bar{p}^2$  is constant over a wide range of Reynolds numbers. We have expressed the pressure ratio in terms of turbulence level (TL):

$$\bar{p}^2 = (TL)^4 q^2.$$

Using an exponential representation of the PSD curve,

$$W_p(f) = W_p(o) e^{-f/f_o},$$

where

$W_p$  = power spectral density,  
 $f$  = natural frequency,

564 105

o = subscript for reference frequency  
e = base of natural logarithms,

we obtain

$$W_p f \leq \bar{p}^2/e.$$

The shape of this PSD curve is very similar to pressure PSD curves based on experimental data. Since  $W_p$  is defined only for positive frequencies, the forcing function as used in the analysis is given by

$$S_p = \bar{p}^2/(2e\bar{f})$$

where  $e = 2.718$ .

Clinch obtained a turbulence level of 0.384; however, to provide more conservative loads on the SSHT, a turbulence level of 0.2 is used.

The RMS pressure value for the design loading provides additional assurance that a representative load is being used. From the curve in Figure 5-11, it is estimated that the RMS value is equal 0.3 psi over the frequency range of 100 to 500 Hz. A conservative axial flow velocity, 50 fps, is used in deriving the pressure loading. The damping ratio used in the analysis is 1% and is supported by test data.

The correlation length ( $\lambda$ ) used in the analysis is 4 inches; this corresponds to the distance from the thermal shield to the SSHT and to the diameter of the SSHT. The correlation length is a measure of coherence in pressure from one point on the structure to another.

The mode shapes of the outer tube for several natural frequencies of the assembly were computed, and results were obtained in terms of RMS displacements for each mode. The normalized displacements from the modal analysis were then scaled to determine the maximum stresses in the assembly. These results are summarized in Table 5-3. Note that the response becomes negligible at the higher frequencies.

#### 5.4.2. Periodic Pressure Fluctuations

Sinusoidal varying pressures from the reactor coolant (RC) pumps have been considered in the analysis of the SSHT. The amplitudes and frequencies of the sinusoidal pressures are shown in Table 5-4. These values were determined

from pressure measurements obtained at a location three pipe diameters downstream from the discharge of an RC pump installed in a large test loop. Since the measured pressures correlated very well across the pipe diameter and along the pipe axis, they are treated in a plane wave fashion. Consequently, pressure differences across the SSHT can be determined by the following conservative method:

It is assumed that any flow effects (velocity, density gradient, etc.) can be neglected. The sonic velocity in the reactor coolant is given by

$$c = \sqrt{\frac{Eg}{\rho}} = \left( \frac{6.5 \times 10^4 \times 386}{45/1728} \right)^{1/2} = 31,040 \text{ in./s}$$

where  
 E = bulk modulus of fluid,  
 g = acceleration of gravity,  
 ρ = density.

The wave length is then given by

$$\lambda = c/f$$

where f = frequency (Hz); for example,

$$\lambda_{20 \text{ Hz}} = 1552 \text{ in./cycle.}$$

This acoustic wavelength is so large (especially at low frequencies) that it is impossible for the tube diameter of the SSHT to see more than a small portion of the whole wavelength at any one time. Consequently, the maximum pressure differential across the tube at any one point in time can be written as

$$\Delta P = P \sin \frac{2\pi d}{\lambda} \quad (\text{see Figure 5-12})$$

where  
 P = peak-to-peak amplitude of incoming wave,  
 d = tube diameter,  
 λ = wavelength.

This can be written as

$$\Delta P = P \sin \frac{2\pi df}{c}$$

564 107

and is of course the amplitude of the harmonic forcing function. It is further assumed that this force is uniform along the axial length of the tube. The magnitude of the sinusoidal pressure wave in the annular region was determined. It is assumed that no losses in pressure amplitude occur as the wave travels along the inlet pipe. As it enters the upper annular region, the wave is assumed to experience no losses, but the pressure magnitude is scaled by the inverse ratio of the sectional area in this annular region to the cross-sectional area of the inlet pipe. To facilitate the analysis, the sectional area is approximated as a frustum of a cone as illustrated in Figure 5-13. This results in a scale factor of 5.7. Since no losses have been assumed across the inlet annulus interface, only the pressures in the frustum region will propagate down and around the annulus. It is assumed the SSHT will be subjected to pressure fluctuations from all the pumps by waves traveling around the annulus. However, in actuality, the pressures will decrease as an inverse function of the distance from the reactor inlet. Furthermore, there is no reason to expect the effects of all the pumps on any tube to be fully additive over the length of the tube. However, to ensure conservative use of the pump-induced pressure fluctuations, the pressure magnitude is taken directly from the inlet region scaled only for the initial area effects. Further, it is assumed that a fully coherent, plane wave impinges on the tube in the tangential direction. No scattering effects are included, and the full differential pressure is applied to the tube rather than integrating the pressure over the tube surface, which would reduce the effective pressure by  $\pi/4$ . The final pressure fluctuations, scaled for the area ratio and wavelength effects, are given in Table 5-5.

#### 5.4.3. Vortex Shedding

The oscillatory lift and drag forces caused by vortex shedding are computed in this section. Vortices are shed from the surveillance holder assembly due to flow crossing the tube normal to its axis. If we take the maximum predicted crossflow velocity of 17.5 fps and apply a conservative upset factor of 1.5, we compute a maximum expected value of 26.25 fps for the crossflow. Figure 5-14 illustrates the design flow velocity distribution. From this we estimate the Reynolds number as

$$Re = \frac{Vd}{\nu} = \frac{26.25}{0.0014 \times 10^{-6}} \times \frac{3.75}{12} = 0.586 \times 10^7$$

564 108

where

- V = crossflow velocity, fps,
- d = characteristic length (tube diameter),
- $\nu$  = Kinematic viscosity, ft<sup>2</sup>/s.

Using this result, we obtain a Strouhal number of 0.300. This, then, defines the frequency of oscillatory lift due to vortex shedding:

$$f_{sh} = \frac{SV}{d} = \frac{0.300 \times 26.25}{3.75/12} = 25.20 \text{ Hz}$$

where

- $f_{sh}$  = vortex shedding frequency,
- S = Strouhal number,
- V = crossflow velocity,
- d = diameter of tube.

There should also be an additional oscillatory driving force at twice this frequency but in the drag (tangential) direction. We obtain the magnitude of the lift (or drag) force from

$$L = \frac{1}{2} \rho V^2 C_L d l$$

or the lift per unit length as

$$\frac{L}{l} = \frac{1}{2} \rho V^2 C_L d.$$

These equations can be used to compute the lift (or drag) forces to be lumped at each node of the computer model.

From Chen<sup>4</sup> we note that the Reynolds number is in a region characterized by boundary instabilities due to the transition from a laminar to a turbulent regime. We expect the boundary layer to be turbulent; hence, we choose a  $C_L$  that lies on the turbulent side of the transition region ( $C_L = 0.2$ ). The frequency of the lift is separated from the lowest natural frequency of the system by nearly 8.1 times, so the load can be essentially considered as static (a magnification factor of 1). The oscillatory drag forces encountered with vortex shedding are typically an order of magnitude lower than those in the lift direction; however, to be conservative, we shall consider these drag forces to be equal in magnitude to and at twice the frequency of the lift force.

The resultant vortex shedding loads can now be computed and applied to the previously described finite element model. Displacements and stresses at lift and drag

frequencies can then be determined. Results of this analysis are presented later. Summarizing the conservatisms used in defining the vortex shedding forces:

1. Design crossflow velocity 1.5 times larger than for normal four-pump operation.
2. Conservative factor of 1.5 applied to specified crossflow velocities from vessel model flow tests.
3. Shedding frequency determined using maximum velocities.
4. Measured RMS  $C_L$  values of less than 0.05 instead of 0.2.
5. Drag forces assumed equal in magnitude to lift forces.

#### 5.4.4. Thermal Shield Excitation

Since the assembly is attached to the thermal shield, it is subjected to the flow-induced vibratory motions of that structure. Table 5-6 gives the frequencies and responses of the thermal shield. These were determined from accelerations of the shield that were measured during preoperational testing of the prototype internals for the 177-fuel assembly plants. A conservative acceleration field of 0.06 g's was determined by using a frequency of 24 Hz and a displacement of 0.001 inch. An inertial load resulting from the 0.06 g's acceleration was applied to the assembly, and the corresponding stresses were determined.

All the frequencies tabulated in Table 5-6 are for modes having a single degree of curvature ( $m=1$ ) in the axial direction. Higher thermal shield modes ( $m=2$ ), which might tend to match the lowest mode shape of the SSHT, are not discernable in the measured data. Thus, it is assumed that there is not enough energy in the higher modes to significantly affect the response of the SSHT assembly.

#### 5.4.5. Endurance Limit Analysis

In general, all hydraulically induced vibratory loadings can be related to the dynamic head, which is a function of the square of the fluid velocity. A good "rule of thumb" engineering analysis is to evaluate the response of the structure in question to an applied loading of 10 times the dynamic pressure,  $\rho V^2/2$ . The resultant stresses are considered to act for an infinite number of cycles and are compared with a material endurance limit to determine structural adequacy. Such an approach is described in detail in BAW-10051<sup>1</sup>

and has proved to be a reliable design tool for structures in severe flow-induced environments.

For a thorough evaluation of the 177-fuel assembly redesigned SSHT, the "endurance limit" analysis was conducted. Figure 5-15 summarizes the results of this analysis, which, for the sake of consistency, were compared with endurance limits given in BAW-10051.

#### 5.5. Seismic Loadings

An acceleration field of 0.90 g's was applied to the SSHT assembly due to the seismic response of the core support assembly (CSA). The "g" level was determined from a CSA beam mode frequency of 8 Hz and a maximum displacement of 0.14 inch. The displacement was conservatively determined from the B&W 205-fuel assembly standard plant OBE response spectra.

An inertial load resulting from 0.90 g's acceleration was applied to the assembly and the corresponding stresses determined.

#### 5.6. Normal and Upset Condition Stress Analysis

This section describes the SSHT stress analysis for normal and upset (seismic) conditions. The previously described thermal and vibratory loadings are included. To facilitate the computation of stresses in the component parts of the SSHT assembly, the NASTRAN finite element model described in section 5.2 was used. Summaries of stress results and ASME Code allowable limits are provided in the following paragraphs. Maximum stresses are reported for the holder tube, the brackets, and the surveillance capsules.

##### 5.6.1. Steady-State Stresses

Steady-state stresses in the SSHT are derived from capsule preload, thermally induced loads, dead weight, and steady drag. The capsule preload is applied by compressing the capsules and stretching the tube. This load was conservatively taken as 10,000 pounds maximum. The thermal stresses result from average temperatures of 596F for the thermal shield and 555F for the tube and capsules. The steady drag load was calculated using a drag coefficient of 1.0 and the load distribution described in section 5.4.3.

The stresses for these conditions are summarized in Table 5-7 (primary + secondary stresses) and Table 5-8 (peak stresses). The results in Table 5-7 include a weld quality factor of 0.65 for the capsule and an area reduction factor of

2.2 for the perforated tube. Table 5-8 includes stress concentration factors of 1.3 (bracket leg geometry), 2.18 (tube perforations), and 2.0 (capsule weld).

#### 5.6.2. Vibrational Stresses

Low-frequency loadings consist of vortex shedding (approximately 50 Hz), operating basis earthquake (about 8 Hz), and thermal shield motions (about 24 Hz). The latter two loadings produce acceleration loadings of 0.90 and 0.06 g, respectively, in the assembly. The stresses caused by these loadings are negligible. The peak stresses due to the combined oscillatory lift and drag caused by vortex shedding are shown below (given in psi):

Bracket	190
Tube	230
Capsule	40

For a 40-year plant life (100% utilization), 50 Hz produces  $6.0 \times 10^{10}$  cycles. The allowable number of cycles for 230 psi is much larger than  $10^{12}$  cycles.

High-frequency loadings consist of the random and periodic pressure fluctuations discussed in sections 5.4.1 and 5.4.2.

The stresses due to random vibrations were determined by ratioing the stresses from the modal analysis (normalized to a unit maximum displacement) to those given in Table 5-2. The resultant maximum RMS stresses are shown in Table 5-9. The usage factor for RMS stress is calculated using the following equation<sup>5</sup>:

$$U = \frac{n}{c} (\sqrt{2}\sigma_s)^b \Gamma\left(1 + \frac{b}{2}\right)$$

where

U = usage factor,

n = number of effective cycles =  $1.26 \times 10^9 f$  for a 40-year design life,

f = natural frequency, Hz,

$\sigma_s$  = RMS stress,

$\Gamma$  = gamma function given in reference 5.

The terms b and c define an S-N curve of the form  $NS^b = c$ . Figure 4-1 yields values of b = 21.854 and  $c = 1.4055 \times 10^{96}$ . Therefore, the usage factor for a given RMS stress level,  $\sigma_s$ , is computed as follows:

564 112

$$U = (5.83 \times 10^{-77}) f \sigma_g^{21.854}$$

The stresses due to pump pressure fluctuations were calculated using a classical frequency response analysis. The pressure amplitudes given in section 5.4.2. were input at the discrete pump frequencies. The resultant peak stresses for the five- and seven-blade pumps are shown in Table 5-10.

It should be noted that the cumulative usage factor for the random and periodic pressure loadings is much less than the allowable value.

Table 5-1. Summary of Temperatures in SSHT-Related Components

Component	$T_{\max}$ , F	$\bar{T}$ , F
<u>1. <math>\theta = 11^\circ</math>, APF = 1.19<sup>(a)</sup></u>		
Thermal shield	611	596
SSHT	555	555
Specimen cladding	558	557
Charpy specimen (worst case)	578	--
<u>2. <math>\theta = 26.5</math>, APF = 0.83</u>		
Thermal shield	594	583
SSHT	555	555
Specimen cladding	555	555
Tensile specimen (min case)	558	--
<u>3. Pressure vessel 1/4T temp = 572F</u>		

(a) APF: azimuthal peaking factor.

564 113

Table 5-2. SSHT Modal Analysis Results

<u>Displacement direction</u>	<u>Natural freq, Hz</u>	<u>Point of max displ't</u>	
		<u>Components</u>	<u>Location</u>
Radial	219	Tube	Top
	245	Capsule	Lower span
	337	Tube	Top
	430	Tube	Lower span
	510	Tube	Upper span
	618	Capsule	Lower span
Tangential	204	Tube	Top
	233	Capsule	Lower span
	315	Tube	Top
	409	Tube	Lower span
	456	Tube	Upper span
	590	Capsule	Upper span

Table 5-3. Maximum RMS Modal Displacements for SSHT Assembly Due to Random Excitation

<u>Direction</u>	<u>Frequency, Hz</u>	<u>Modal displacement, mils RMS</u>
Radial	219	0.65
	245	0.87
	337	0.19
	430	0.05
Tangential	204	0.82
	233	1.14
	315	0.33
	409	0.09

564 114

Table 5-4. Pressure Fluctuations Measured in Five-Vane Bingham Pump Test Loop

Velocity of sound (c) in coolant at 550F, in./s - fps 31,040 - 2587

$$\lambda = c/f; \quad f = \text{frequency, Hz}$$

Frequency, Hz	$\lambda$ , in.	Pump pressure, <sup>(a)</sup> psi
20	1552	0.23
40	776	0.17
100	310	0.62
140	222	(b)
200	155	4.75
280	111	(b)
300	103	0.48
400	78	3.08
420	74	(b)
560	55	(b)

(a) Peak-to-peak.

(b) Data not available for seven-vane pumps.

564 115

Table 5-5. Periodic Pressure Fluctuations  
Used in SSHT Analysis

<u>Pump manufacturer</u>	<u>No. of impeller vanes</u>	<u>Shaft and BPF, Hz</u>	<u>Pressure, psi</u>
Westinghouse	7	20	NA <sup>(a)</sup>
		40	
		140	
		280	
		420	
		560	
Byron-Jackson	5	20	NA <sup>(a)</sup>
		40	
		100	
		200	
		300	
		400	
Bingham	5	20	$6.1 \times 10^{-4}$
		40	$9.0 \times 10^{-4}$
		100	$8.2 \times 10^{-3}$
		200	$1.3 \times 10^{-1}$
		300	$1.9 \times 10^{-2}$
		400	$1.6 \times 10^{-1}$

(a) Pressures from Bingham test used at these frequencies.

564 116

Table 5-6. Structural Excitations From Thermal Shield

<u>Significant frequencies, Hz</u>	<u>Amplitude, mils</u>
9.0	< 1
11.0	< 1
12.2	< 1
15.0	< 1
23.7	< 1

Notes: No magnification because of wide separation between exciting and natural frequencies.

Maximum acceleration induced by thermal shield on assembly is 0.06 g at  $f = 24$  Hz.

Table 5-7. Steady-State Primary Plus Secondary Stresses

<u>Load</u>	<u>Primary + secondary stress, psi</u>		
	<u>Bracket</u>	<u>Tube</u>	<u>Capsule</u>
Thermal	26,070	1,130	2,750
Tube preload	-11,860	7,820	-14,920
Steady drag	530	380	-110
Dead weight	Negligible	Negligible	Negligible
Total	14,740	9,330	-12,280

ASME Code allowable stress = 50,550 psi ( $3 S_m$ ).

564 117

Table 5-8. Steady-State Peak Stresses

<u>Load</u>	<u>Peak stress, psi</u>		
	<u>Bracket</u>	<u>Tube</u>	<u>Capsule</u>
Thermal	33,890	2,460	3,580
Tube preload	-15,420	17,050	-19,400
Steady drag	690	830	-140
Dead weight	Negligible	Negligible	Negligible
Total	19,160	20,340	-15,960

Maximum cycles = 5,000 (thermal)

Allowable cycles for 20,340 psi = 80,000

Table 5-9. Stresses Due to Random Vibration Loadings

<u>Frequency, Hz</u>	<u>Maximum RMS stress, psi</u>			<u>Usage factor for max stress (U)</u>
	<u>Bracket</u>	<u>Tube</u>	<u>Capsule</u>	
204	720	1140	740	$7.6 \times 10^{-8}$
219	290	870	870	$2.2 \times 10^{-10}$
233	1000	1160	1680	$4.2 \times 10^{-4}$
245	340	720	1340	$3.1 \times 10^{-6}$
315	420	270	690	$2.0 \times 10^{-12}$
337	90	200	400	$1.4 \times 10^{-17}$
409	120	300	140	$3.3 \times 10^{-20}$
430	30	180	90	$4.9 \times 10^{-25}$

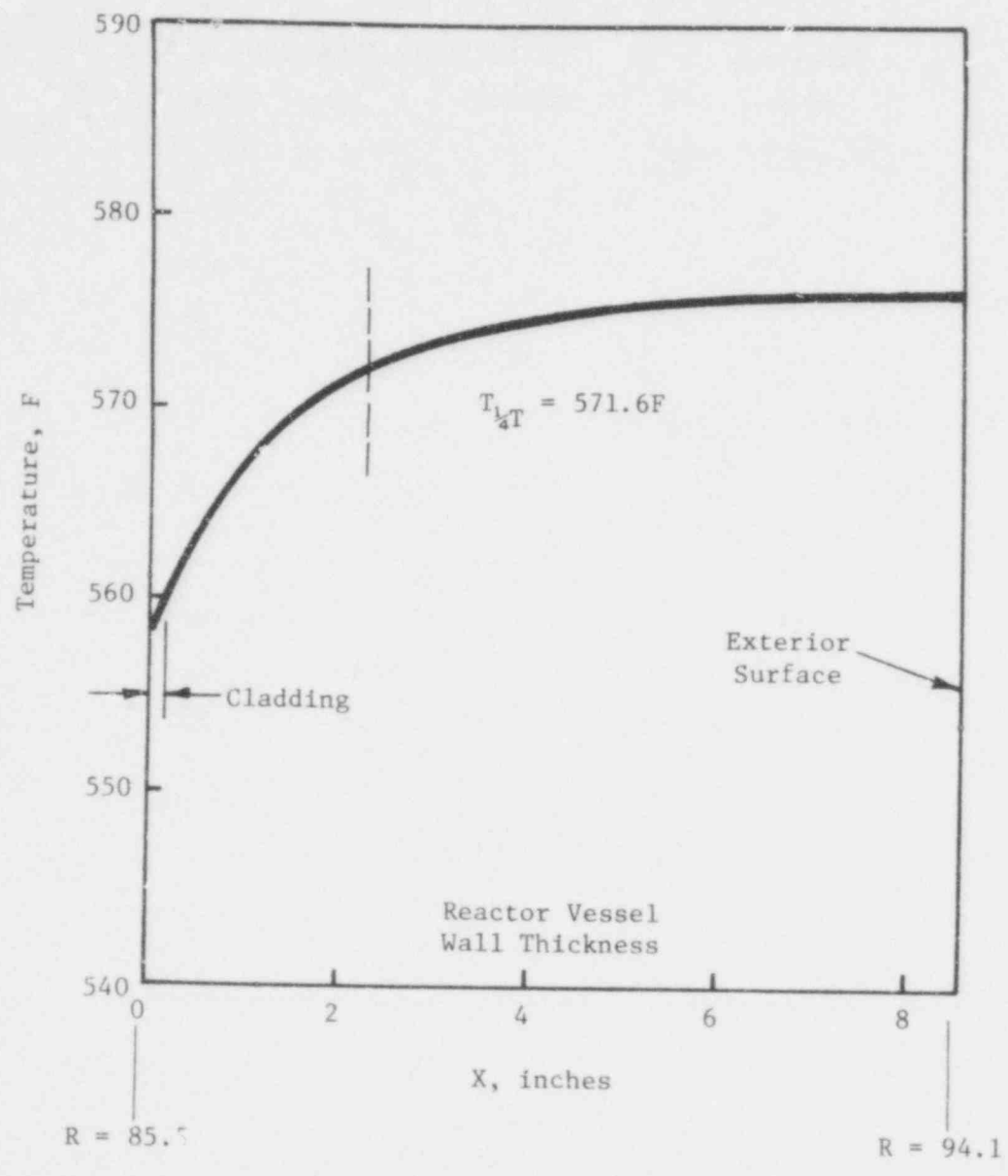
564 118

Table 5-10. Stresses Due to Periodic Pump Pressure Loadings

Frequency, Hz	Peak stress amplitude, psi		
	Bracket	Tube	Capsule
<u>Five-blade pump</u>			
100	17	4	2
200	103	82	102
300	27	24	34
400	338	352	561
<u>Seven-blade pump</u>			
20	--	--	--
40	--	--	--
140	4	6	3
280	146	154	135
420	48	108	71
560	92	99	71

564 119

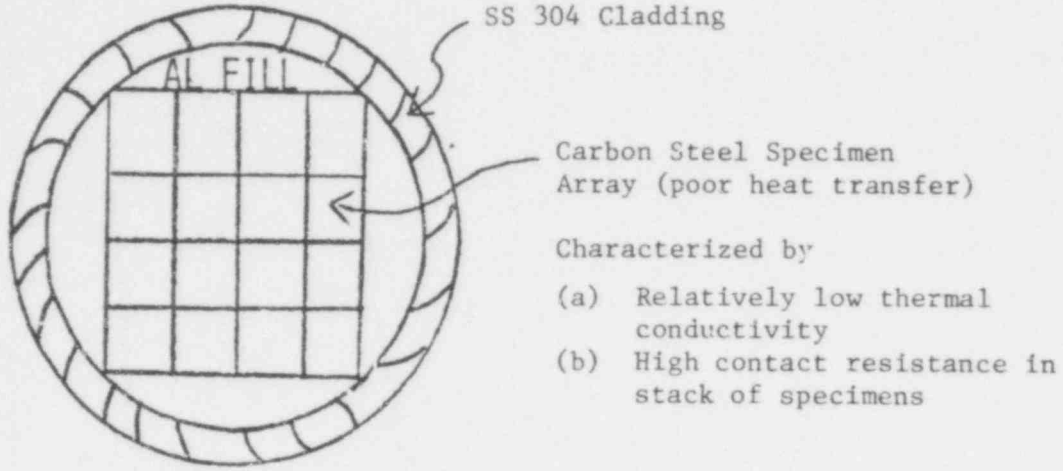
Figure 5-1. 177-FA Pressure Vessel Temperature Distribution Due to Gamma Heating



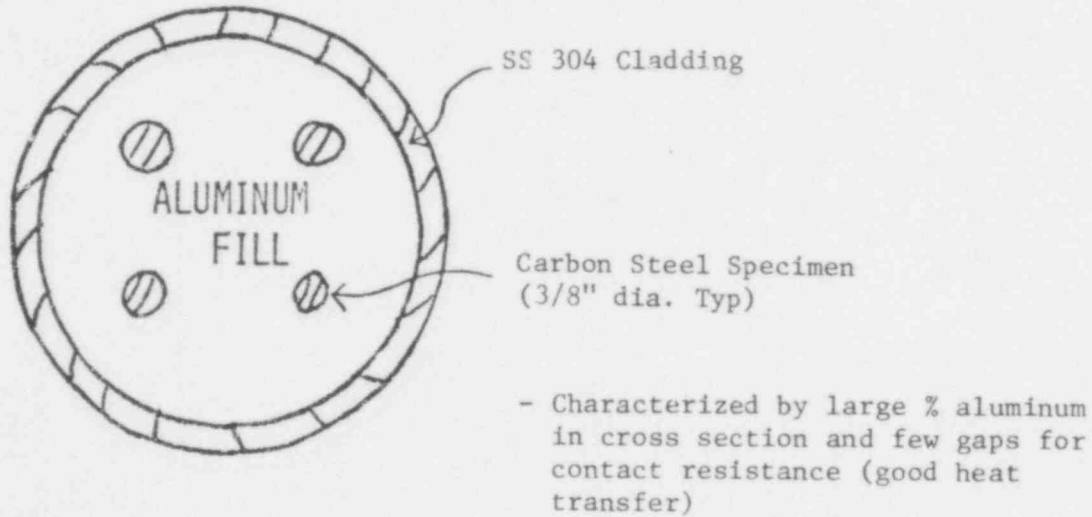
564 120

Figure 5-2. Surveillance Specimen Configurations

a. Charpy Specimen

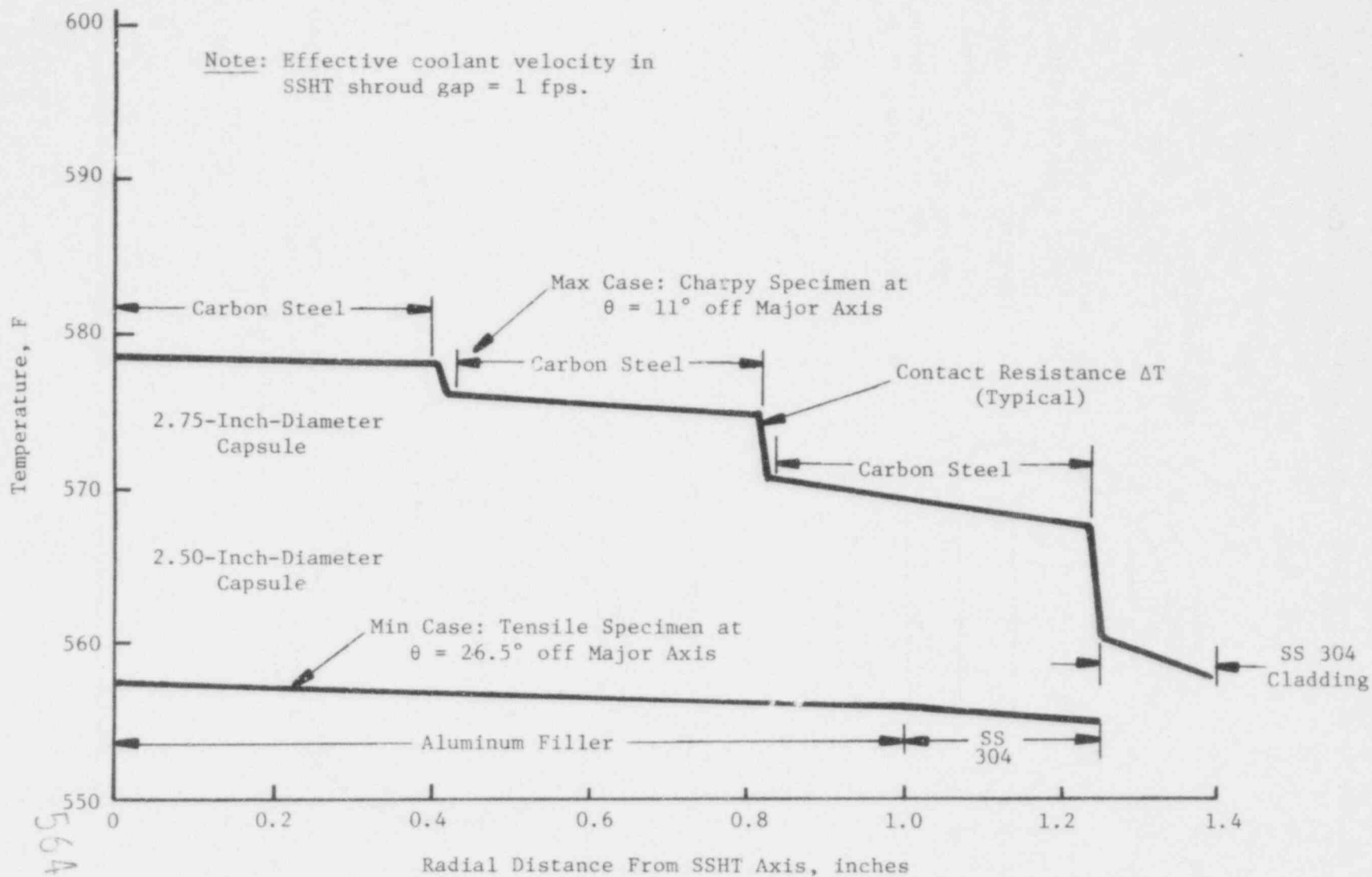


b. Tensile Specimen



564 121

Figure 5-3. Surveillance Specimen Temperature Study

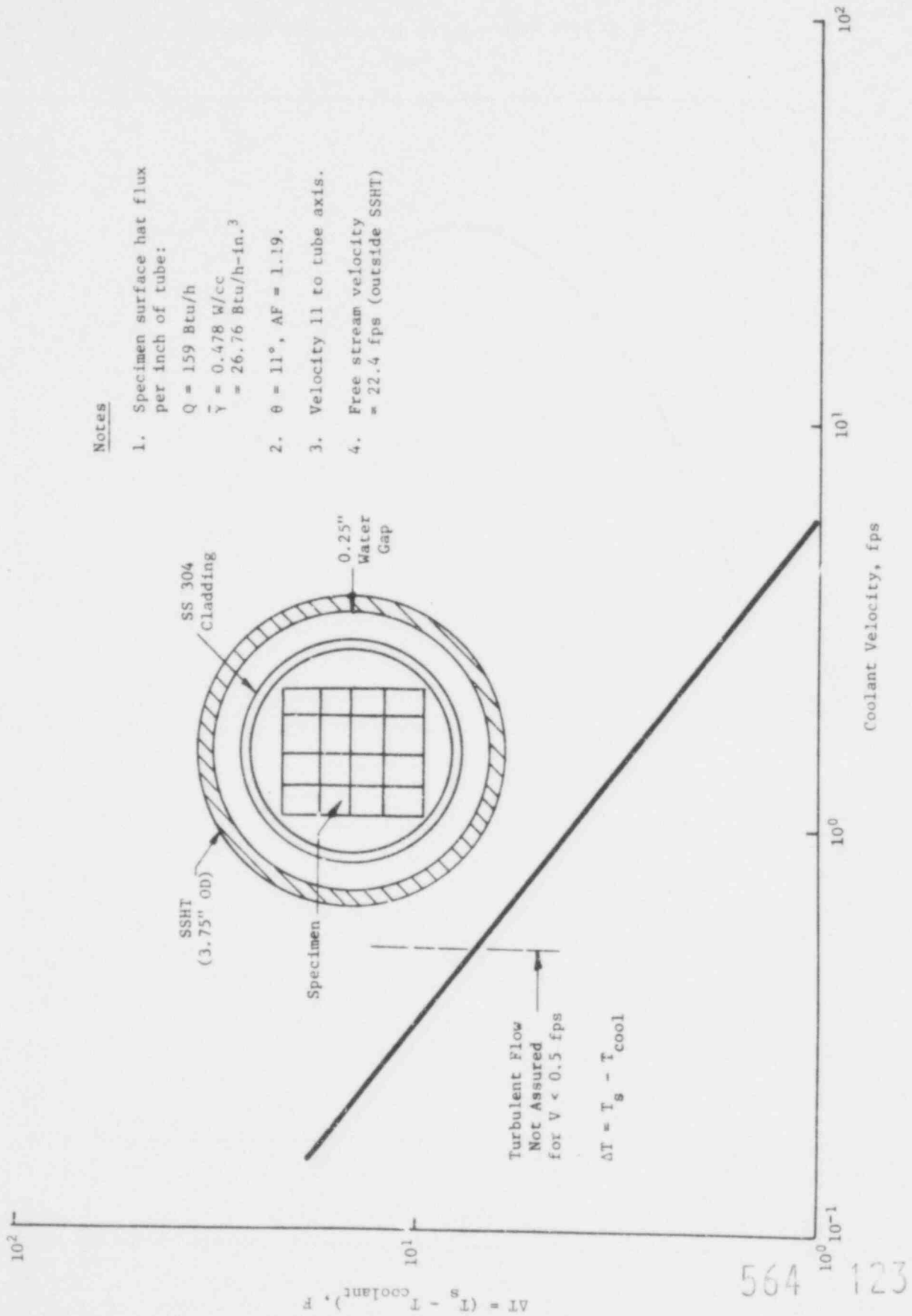


5-22

Babcock & Wilcox

564  
122

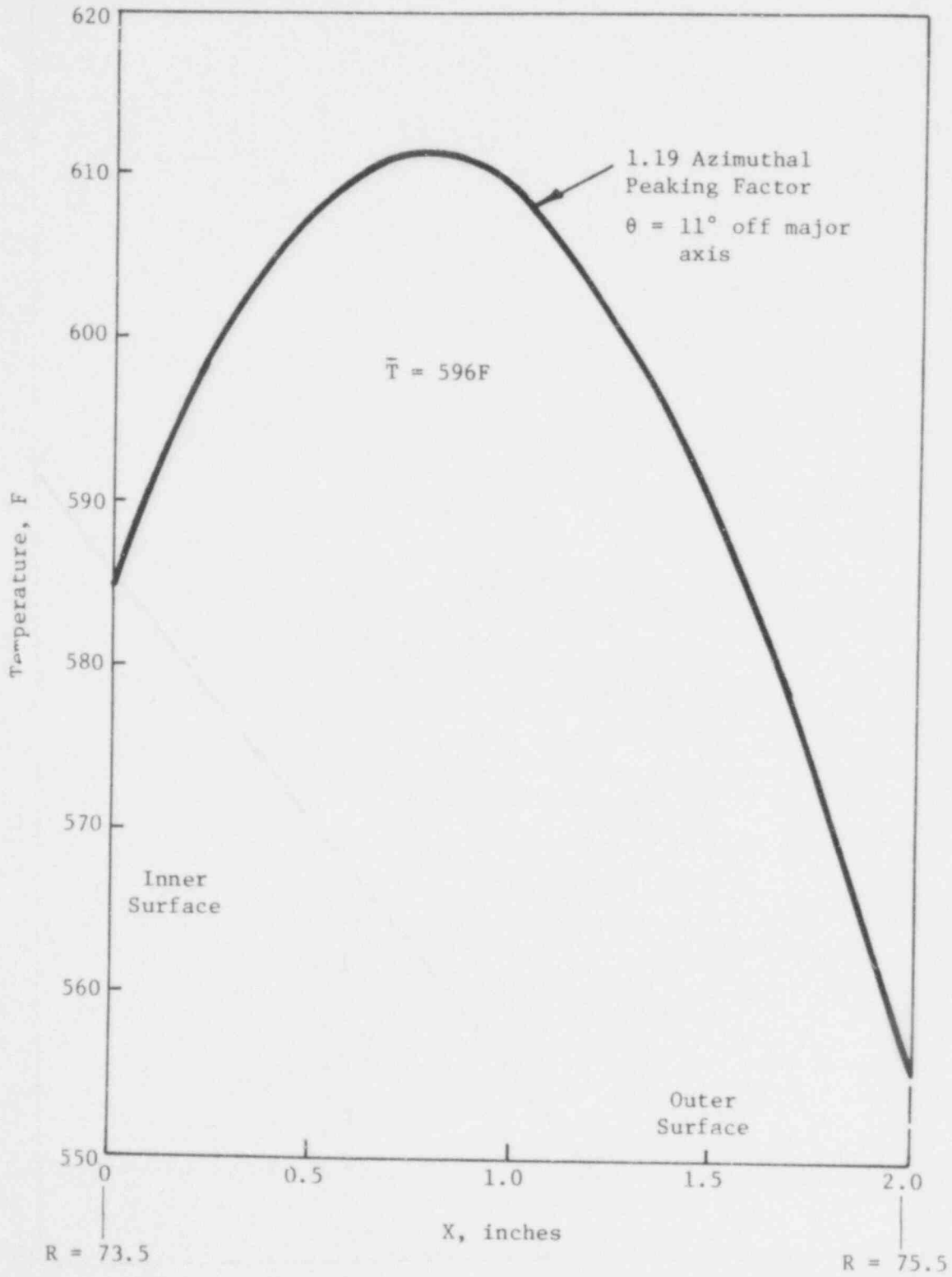
Figure 5-4. Surveillance Specimen Surface Temperature Vs Flow Velocity



Notes

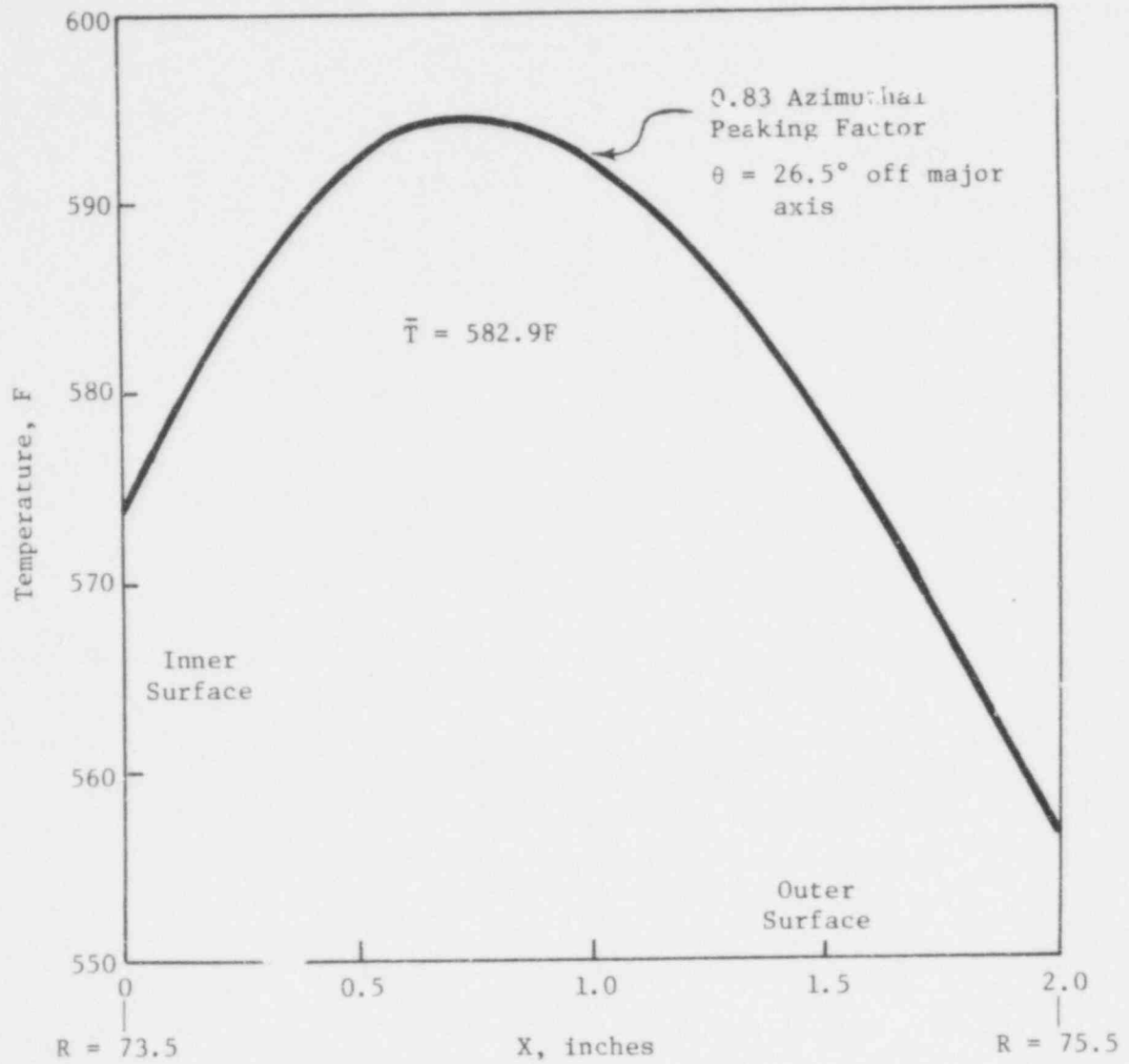
1. Specimen surface heat flux per inch of tube:  
 $Q = 159$  Btu/h  
 $\bar{y} = 0.478$  W/cc  
 $= 26.76$  Btu/h-in.<sup>3</sup>
2.  $\theta = 11^\circ$ , AF = 1.19.
3. Velocity 11 to tube axis.
4. Free stream velocity = 22.4 fps (outside SSHT)

Figure 5-5. Temperature Distribution in 177-FA Thermal Shield,  $\theta = 11^\circ$



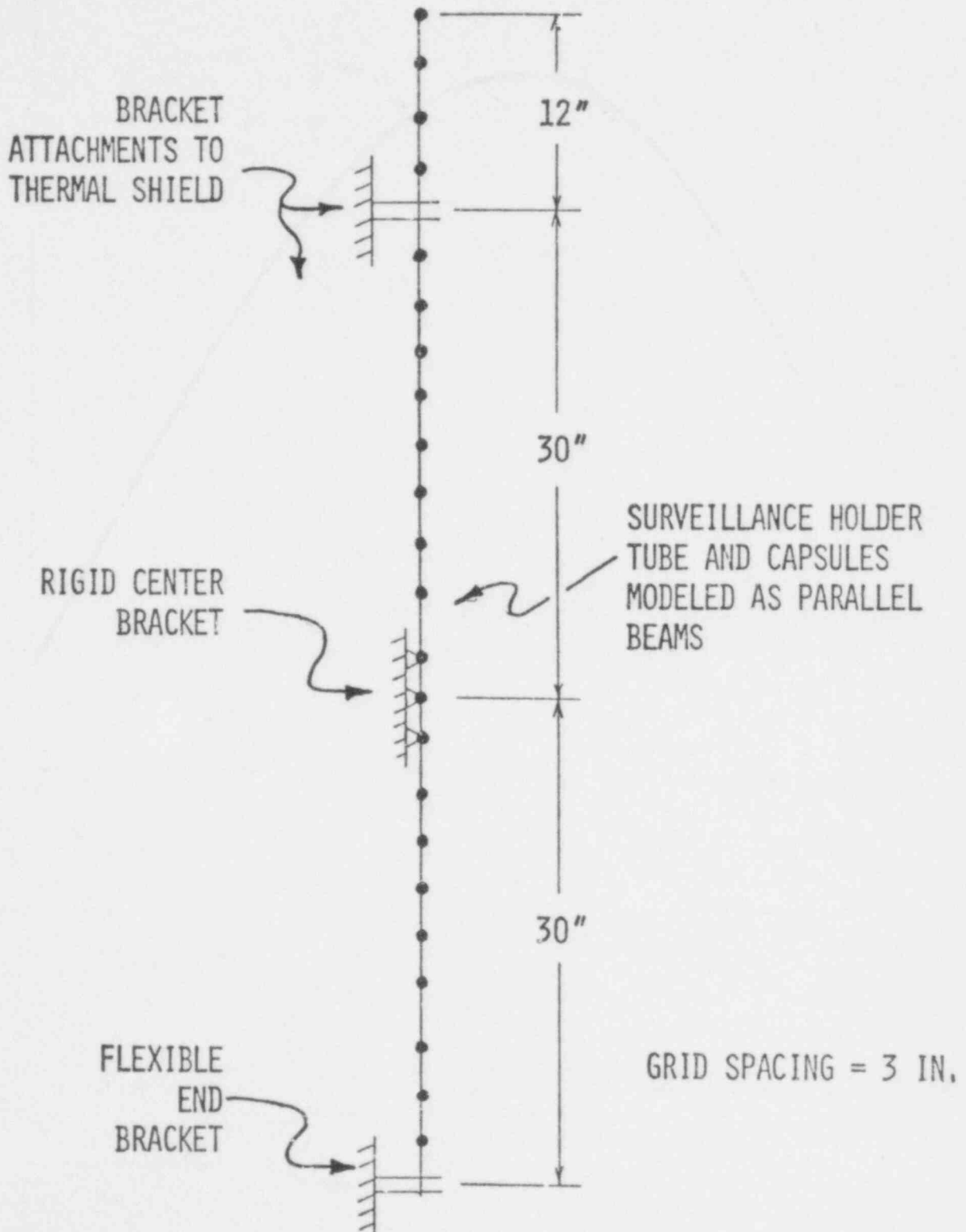
564 124

Figure 5-6. Temperature Distribution in 177-FA Thermal Shield,  $\theta = 26.5^\circ$



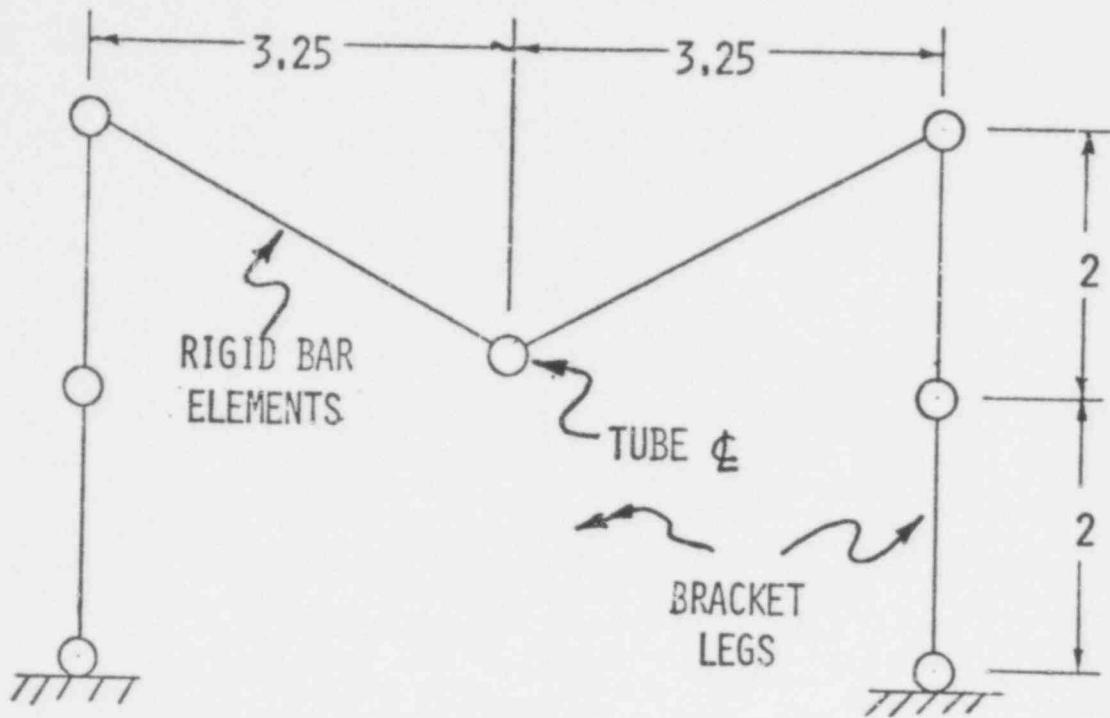
564 125

Figure 5-7. Finite Element Beam Model of SSHT and Support Brackets



564 126

Figure 5-8. Finite Element Beam Model of SSHT Support Brackets



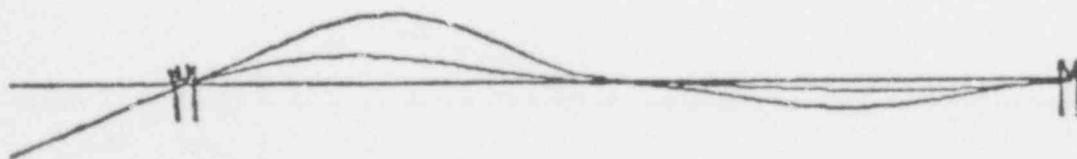
Dimensions in inches.

564 127

Figure 5-9. First Fundamental Mode Shape of SSHT and Capsules (Tangential Motion  $F = 204$  Hz)

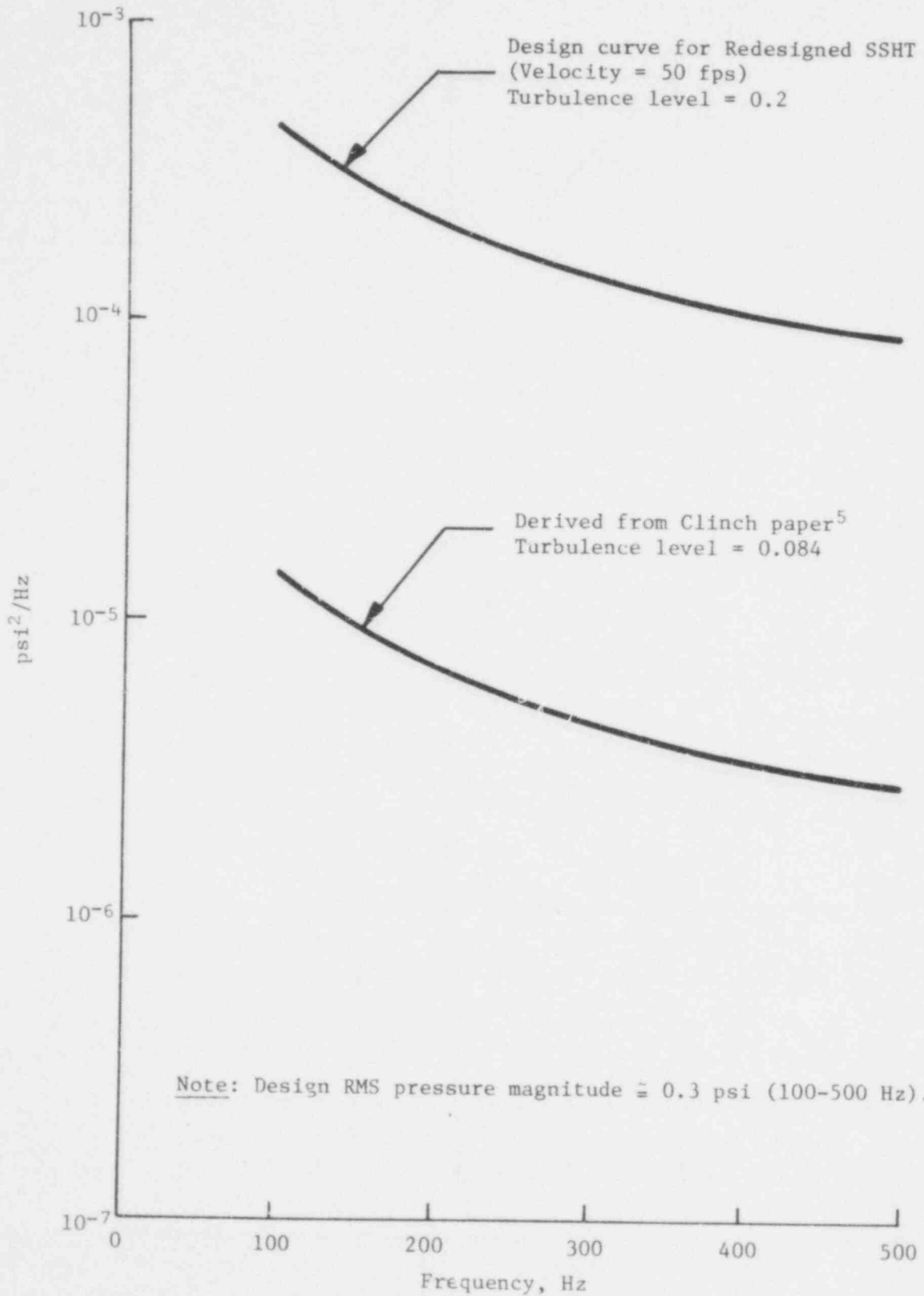


Figure 5-10. Second Fundamental Mode Shape of SSHT and Capsules (Radial Motion  $F = 219$  Hz)



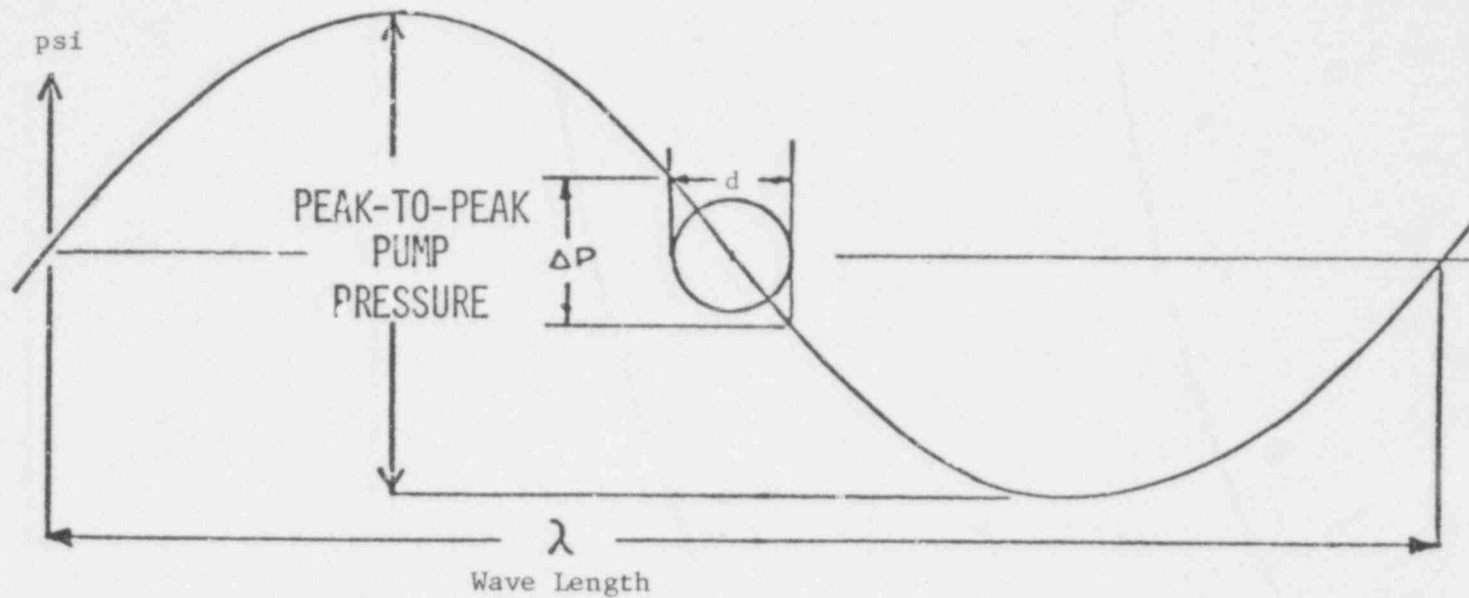
564 128

Figure 5-11. Random Pressure Loading Functions



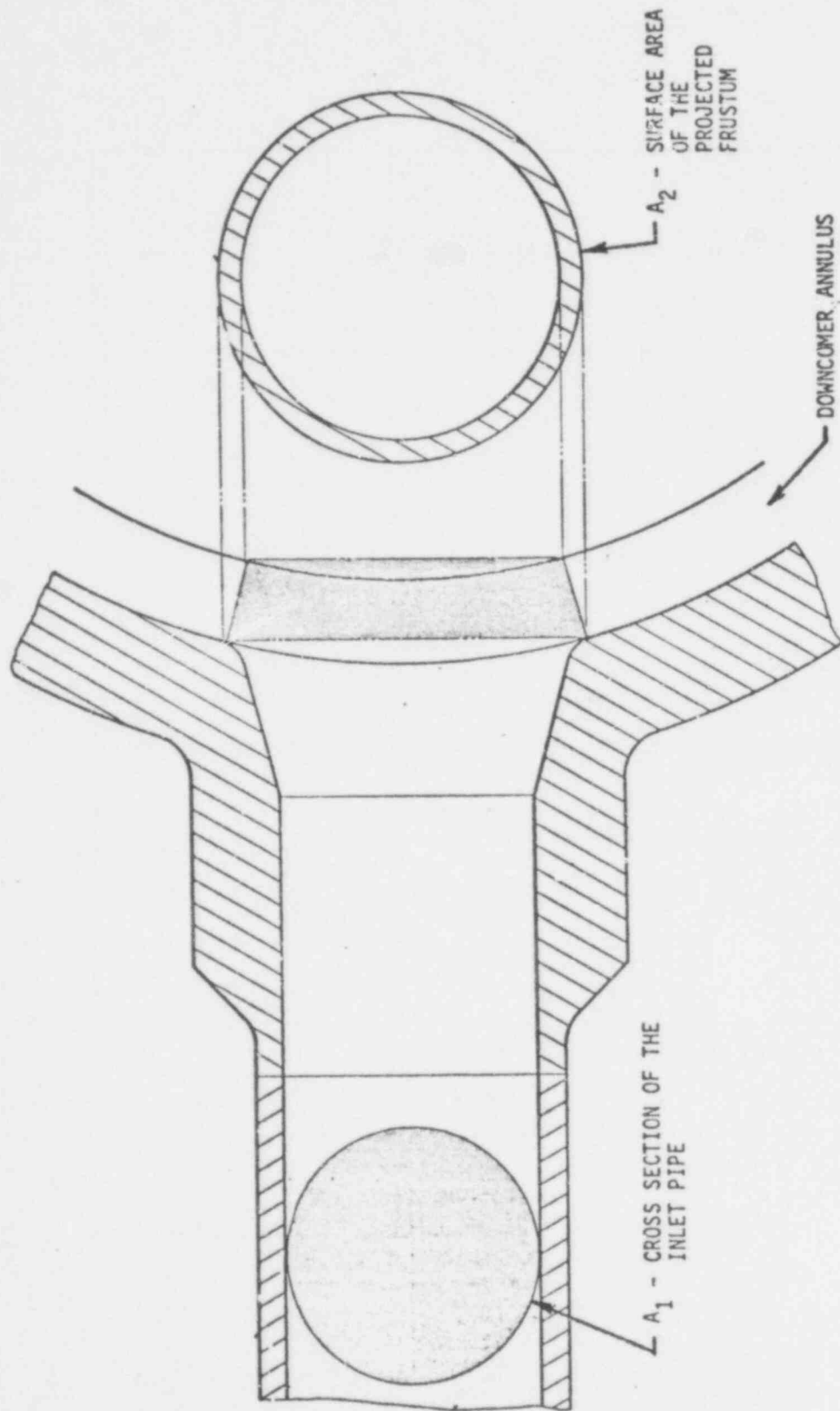
564 129

Figure 5-12. Superposition of Pump Pressure Wave on SSHT



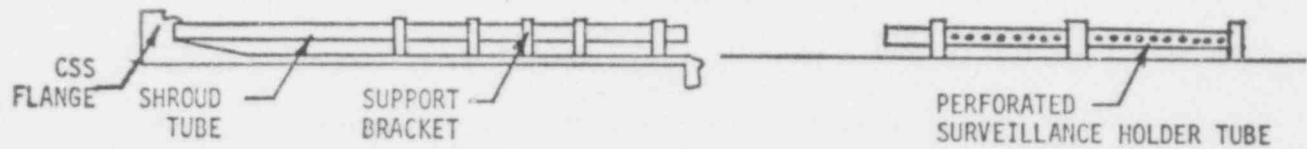
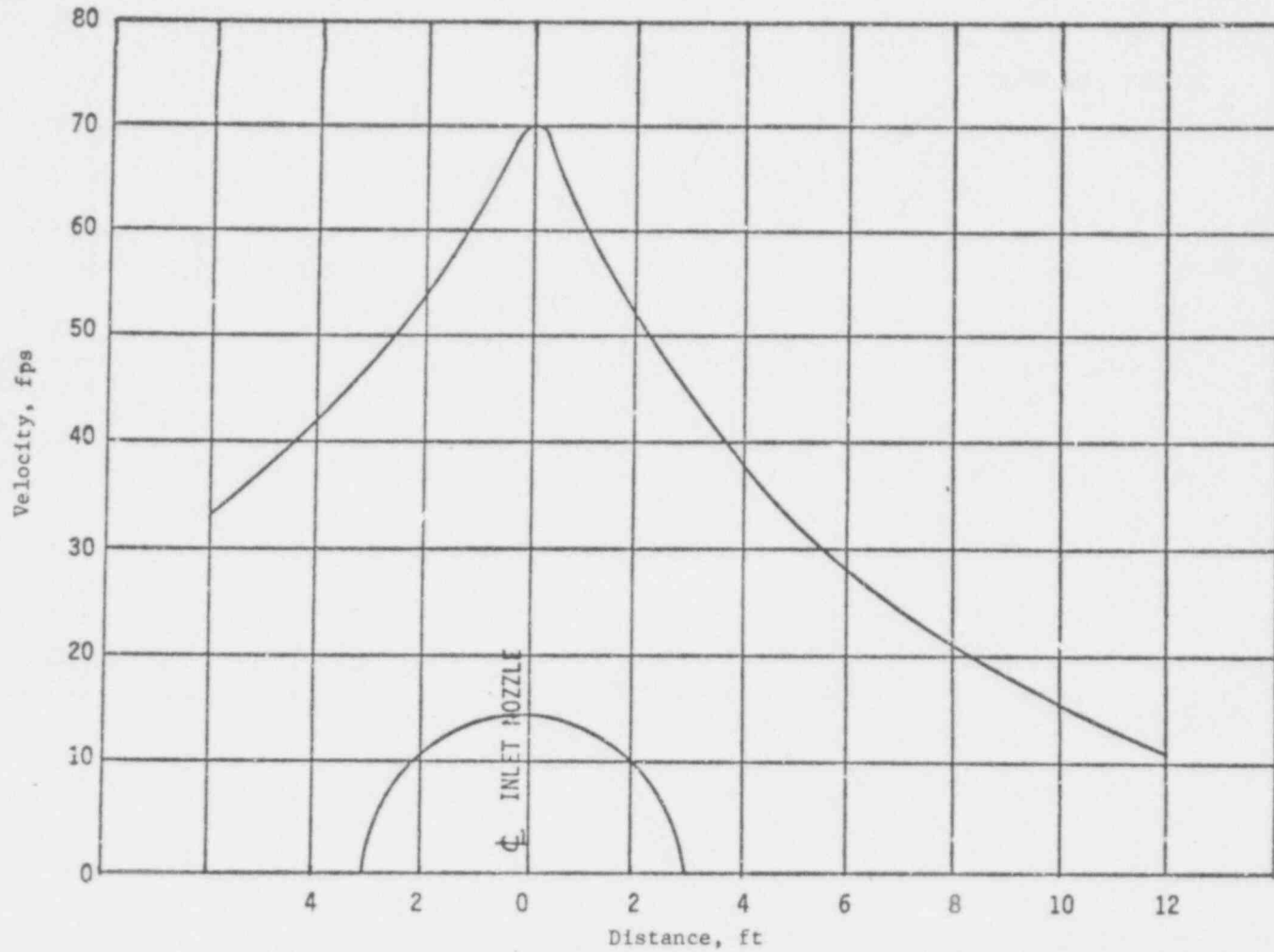
A = Tube diameter, 3.75 in.

Figure 5-13. Dispersion of Pump Pressure Pulsation at Reactor Vessel Inlet



564 131

Figure 5-14. Design Crossflow Velocity Distribution for 177-FA Redesigned SSHT



5-32

Babcock & Wilcox

564 152

Figure 5-15. Results of Endurance Limit Analysis  
of 177-FA SSHT

<u>Loading</u>	<u>Peak stress amplitude, psi</u>		
	<u>Bracket</u>	<u>Tube</u>	<u>Capsule</u>
10 $\frac{\rho V^2}{2g}$ (Uniformly applied over SSHT length)	9,500	11,500	2,000

Endurance limit = 18,000 psi (BAW-10051)

564 133

#### REFERENCES

- <sup>1</sup> Design of Reactor Internals and Incore Instrument Nozzles for Flow-Induced Vibration, BAW-10051, September 1972.
- <sup>2</sup> R. J. Fritz, "The Effects of Liquids on the Dynamic Motions of Immersed Solids," Journal of Engineering for Industry, February 1972.
- <sup>3</sup> J. M. Clinch, "Measurements of the Wall Pressure Field at the Surface of a Smooth-Walled Pipe Containing Turbulent Water Flow," Journal of Sound & Vibration (1969).
- <sup>4</sup> Y. N. Chen, "Fluctuating Lift Forces of the Karman Vortex Streets on Single Circular Cylinders and in Tube Bundles, Part 2," Journal of Engineering for Industry, ASME, May 1972.
- <sup>5</sup> S. H. Crandall and W. D. Mark, Random Vibration in Mechanical Systems, Academic Press (1963).

564 134